

Title

Assessing functional connectivity differences and work-related fatigue in surviving COVID-negative patients.

Running title

Functional Alterations and Fatigue in COVID

Author Names and Affiliations

Rakibul Hafiz ‡¹, Tapan Kumar Gandhi ‡², Sapna Mishra², Alok Prasad³, Vidur Mahajan⁴, Benjamin H. Natelson⁵, Xin Di¹, Bharat B. Biswal*¹

1: Department of Biomedical Engineering, New Jersey Institute of Technology (NJIT), 323 Dr Martin Luther King Jr Blvd, Newark, NJ 07102, USA

2: Department of Electrical Engineering, Indian Institute of Technology (IIT), Block II, IIT Delhi Main Rd, IIT Campus, Hauz Khas, New Delhi, Delhi 110016, India

3: Internal Medicine, Irene Hospital & Senior Consultant Medicine, Metro Heart and Super-specialty Hospital, New Delhi, India

4: Centre for Advanced Research in Imaging, Neuroscience & Genomics, Mahajan Imaging, New Delhi, India

5: Pain and Fatigue Study Center, Department of Neurology, Icahn School of Medicine at Mount Sinai, NY, USA

‡: The authors contributed equally for this project as first authors.

* Corresponding Author e-mail

bharat.biswal@njit.edu

Number of pages: 17

Number of figures: 3

Number of Words

Abstract: 175

Introduction: 1103

Discussion: 868

Conflict of interest statement: The authors declare no competing financial interests.

Acknowledgements: This study was supported by an NIH grant (R01AT009829).

1 **Abstract**

2 The Coronavirus Disease 2019 (COVID-19) has affected all aspects of life around the
3 world. Neuroimaging evidence suggests the novel coronavirus can attack the central
4 nervous system (CNS), causing cerebro-vascular abnormalities in the brain. This can lead
5 to focal changes in cerebral blood flow and metabolic oxygen consumption rate in the
6 brain. However, the extent and spatial locations of brain alterations in COVID-19 survivors
7 are largely unknown. In this study, we have assessed brain functional connectivity (FC)
8 using resting-state functional MRI (RS-fMRI) in 38 (25 males) COVID patients two weeks
9 after hospital discharge, when PCR negative and 31 (24 males) healthy subjects. FC was
10 estimated using independent component analysis (ICA) and dual regression. When
11 compared to the healthy group, the COVID group demonstrated significantly enhanced
12 FC in the *basal ganglia* and *precuneus* networks (*family wise error (fwe) corrected, $p_{fwe} <$*
13 *0.05*), while, on the other hand, reduced FC in the *language* network (*$p_{fwe} < 0.05$*). The
14 COVID group also experienced higher fatigue levels during work, compared to the healthy
15 group (*$p < 0.001$*). Moreover, within the *precuneus* network, we noticed a significant
16 negative correlation between FC and fatigue scores across groups (*Spearman's $\rho = -$*
17 *0.47, $p = 0.001$, $r^2 = 0.22$*). Interestingly, this relationship was found to be significantly
18 stronger among COVID survivors within the left *parietal lobe*, which is known to be
19 structurally and functionally associated with fatigue in other neurological disorders.

20 **Keywords:** COVID, Functional Connectivity, ICA, Fatigue, RS-fMRI

21 **Significance Statement**

22 Early neuroimaging studies have mostly focused on structural MRI imaging to report brain
23 abnormalities in acutely ill COVID-19 patients. It is not clear whether functional
24 abnormalities co-exist with structural alterations in patients who have survived the
25 infection and have been discharged from the hospital. A few recent studies have emerged
26 which attempted to address the structural/functional alterations. However, further
27 investigations across different sites are necessary for more conclusive inference. More
28 importantly, fatigue is a highly prevalent symptom among COVID survivors, therefore, the
29 relations of brain imaging abnormalities to fatigue should be investigated. In this study,
30 we try to address these gaps, by collecting imaging data from COVID survivors, now PCR
31 negative, and healthy subjects from a single site – the Indian Institute of Technology (IIT),
32 Delhi, India. Furthermore, this is a continuation of an ongoing study. We have recently
33 shown structural abnormalities and stronger gray matter volume (GMV) correlates of self-
34 reported fatigue in this group of COVID survivors compared to healthy subjects (Hafiz et
35 al., 2022).

36 **Introduction**

37 The novel coronavirus pandemic has taken more than 4.5 million lives across the globe
38 ((WHO), 2020). Vaccinations and mask mandates have reduced the spread; however,
39 new variants have badly affected densely populated countries, a prime example being,
40 India. Recent evidence shows, Severe Acute Respiratory Syndrome Coronavirus 2
41 (SARS-CoV-2) can attack the central nervous system (CNS). Clinical MRI from early

42 pandemic reports show cerebrovascular and inflammatory vascular pathologies – acute
43 infarcts, posterior reversible encephalopathy syndrome, microhemorrhages etc. (Gulko
44 et al., 2020; Keller et al., 2020; Nicholson et al., 2020). It is deeply concerning that
45 abnormal fluid-attenuated inversion recovery (FLAIR) uptakes were ubiquitously found in
46 most major brain lobes – frontal, parietal, occipital, temporal, insular and cingulate cortex
47 (Kandemirli et al., 2020), as well as in the sub-cortical systems (Paterson et al., 2020).
48 These clinical cases led to recent studies with more emphasis on group level structural
49 differences (Douaud et al., 2021; Duan et al., 2021; Qin et al., 2021). We have also shown
50 structural alterations in the same group of patients being investigated in the current study
51 (Hafiz et al., 2022). Whether brain pathologies in these survivors also induce functional
52 brain alterations, need to be investigated.

53 To assess functional brain alterations in COVID survivors, functional magnetic
54 resonance imaging (fMRI) can be implemented. fMRI is sensitive to changes in blood
55 oxygen level dependent (BOLD) signal (Ogawa et al., 1990). Cerebrovascular
56 pathologies in hospitalized COVID patients can modulate blood flow and neural
57 metabolism in the brain. This can lead to abnormal BOLD activity across brain regions,
58 causing alterations in temporal synchronization or functional connectivity (FC) (De Luca
59 et al., 2006; Fox et al., 2005; Fox et al., 2006; Friston, 1994; Friston et al., 1993;
60 Greicius et al., 2003), typically estimated in resting state fMRI (RS-fMRI) among other
61 modalities (Horwitz, 2003). The earliest RS-fMRI study (Biswal et al., 1995) and
62 subsequent studies interpreted FC as information sharing among distinct regions that
63 are temporally synchronized (Cole et al., 2010; De Luca et al., 2006; Fox et al., 2005;
64 Fox et al., 2006; Greicius et al., 2003; Kalcher et al., 2012; Meier et al., 2012). FC can

65 be used to generate robust functional networks (FNs) of the human brain. Independent
66 Component Analysis (ICA) is a popular data driven technique that decomposes the
67 brain voxels into distinct FNs based on the similarity of time courses (McKeown et al.,
68 1998). The ICA-derived large-scale resting-state networks (RSNs) have local and higher
69 level associative hierarchy (Yeo et al., 2011) and replicate highly reproducible activation
70 maps across subjects (Smith et al., 2009).

71 Distributed brain pathologies in hospitalized survivors can affect multiple FNs. Based on
72 earlier evidence (Matsuda et al., 2004; McCray et al., 2007), it is likely the source of
73 neuro-invasion is the olfactory pathways. The current COVID literature also shows
74 abnormalities in the olfactory system (Esposito et al., 2022; Ismail & Gad, 2021;
75 Laurendon et al., 2020; Niesen et al., 2021; Politi et al., 2020). The virus can
76 subsequently stay and cause pathologies by migrating throughout the brain post
77 infection (Daniel et al., 2022). Therefore, it is possible that most FNs are affected and
78 ideally, they should all be investigated. However, to avoid multiple testing complications
79 and based on our recent study (Hafiz et al., 2022) and current literature findings, we
80 focused on FC alterations primarily in five relevant networks – the *basal ganglia*,
81 *precuneus*, *language* and *bilateral somatosensory* networks.

82 The *basal ganglia* is a major hub for projections to and from the cortex and has
83 neuronal connections to the olfactory system (Amunts et al., 2005; Soudry et al., 2011).
84 Recently, we have shown higher GMV within the *basal ganglia* among the same group
85 of survivors in this study (Hafiz et al., 2022). *Precuneus* is a major constituent of *default*
86 *mode network (DMN)*, involved in a multitude of functions including visuo-spatial,
87 memory retrieval, self-referential and switching processes during goal-oriented task

88 (Cavanna & Trimble, 2006; Freton et al., 2014). Reduced FC was reported within *DMN*
89 and between *DMN* and *salience (SAL)* networks in unresponsive COVID survivors
90 (Fischer et al., 2021). Investigating the *precuneus* network may be important for fatigue
91 and attention related deficits among survivors. The *somatosensory* network processes
92 several body related stimuli (Favaro et al., 2012; Kang et al., 2018; Lavagnino et al.,
93 2014) which may relate to symptoms experienced by survivors such as loss in appetite,
94 depression, and sleep disorder among others. The *language* network consists of
95 regions from the *inferior frontal* and *middle temporal gyri (IFG, MTG)*. Duan and
96 colleagues have shown structural abnormalities specifically within the *IFG* and *MTG*
97 regions in COVID survivors (Duan et al., 2021). The *language* network also comprises
98 *cerebellar* regions where both structural abnormalities (Fadakar et al., 2020; Malayala et
99 al., 2021), as well as, enhanced dynamic functional connectivity with *sensorimotor*
100 network have been reported among survivors (Fu et al., 2021).

101 Behaviorally, many COVID survivors experience a sequela of symptoms (Logue et al.,
102 2021; Peluso et al., 2021; Tabacof et al., 2020), now commonly called 'Long COVID',
103 which point to brain as the responsible organ. Fatigue, lack of attention, anxiety,
104 memory loss, delayed recovery of smell and/or taste, muscle pain and stress are
105 commonly reported symptoms. Most contemporary neuroimaging studies have mainly
106 focused on brain correlates of post-traumatic stress syndromes (Benedetti et al., 2021;
107 Fu et al., 2021). On the other hand, several others have attempted to use FC as a
108 neurobiological indicator of higher stress levels (Liu et al., 2021; Perica et al., 2021),
109 depression (Zhang et al., 2022) and negative affect (Xiao et al., 2021) among healthy
110 subjects before and after the pandemic. Despite fatigue being the most frequently

111 reported symptom, very little is known of its brain related effects among survivors. In our
112 recent investigation (Hafiz et al., 2022), we also observed a stronger positive correlation
113 between GMV and work-related fatigue within the *precuneus*, *posterior cingulate cortex*
114 and *superior parietal lobule*. We expect to see similar relationship of FC and work-
115 related within the *precuneus network*.

116 We first apply ICA in RS-fMRI data to estimate FC in healthy controls (HCs) and COVID
117 survivors using group ICA and dual regression (C.F. Beckmann, 2009; Filippini et al.,
118 2009) to test our hypothesis that surviving COVID-negative patients demonstrate
119 altered FC in the *basal ganglia*, *precuneus*, *somatosensory* and *language* networks.
120 Using a self-reported fatigue questionnaire on a scale of 0-5, we further hypothesized
121 that the COVID group is more susceptible to fatigue during work. We also apply a
122 multiple linear regression model to test the hypothesis that FC within the *precuneus*
123 network demonstrate stronger correlation with fatigue compared to HCs.

124 **Materials and Methods**

125 **Participants**

126 This is a continuation of our recent work using the same sample groups where structural
127 brain alterations were reported (Hafiz et al., 2022). 47 COVID patients and 35 HCs were
128 recruited from a single site located at Indian Institute of Technology (IIT), Delhi, India. 9
129 COVID and 4 HC subjects were removed during quality control and motion assessment,
130 leaving with an effective sample of 38 (25 males) COVID and 31 (24 males) HC. The
131 COVID subjects were scanned two weeks after they were released from the hospital

132 when confirmed to be COVID-negative upon polymerase chain reaction (PCR) retesting.

133 During scanning, all protocols were strictly followed based on the Institutional Review

134 Board (IRB) guidelines at the Indian Institute of Technology (IIT), Delhi, India.

135 The patients in this study were recruited from a much larger cohort who were admitted

136 and assessed at the Metro Heart and Super-specialty Hospital, New Delhi, India. The

137 patient evaluation and classification was based on illness severity data derived from a

138 database of 2,538 COVID patients from May to December 2020. 24% of this sample did

139 not require O₂, 40% required O₂, 22% required Continuous Positive Airway Pressure

140 (CPAP); and 14% were intubated. This 14% of intubated patients were excluded from the

141 recruitment process in the current study.

142 Of the remaining patients, 333 needed CPAP to raise O₂ levels; 333 needed nasal O₂ to

143 raise O₂ levels; and 334 were admitted but did not need supplemental O₂. The sample of

144 47 COVID subjects constituting the COVID group in this study were collected from this

145 cohort (those who agreed to participate in this ongoing study so far). Patients were

146 recruited two weeks after discharge, after becoming PCR negative. Any subject from the

147 healthy group who has experienced fever, cough or flue like symptoms in the two weeks

148 prior to scan, were removed from the study. All healthy subjects also had to undergo a

149 PCR test to assure that they had not been infected in the recent past. We used a

150 questionnaire to record symptoms the survivors have experienced during hospitalization

151 (see Figure S1 in the Supplementary Materials) and an additional questionnaire to

152 quantify fatigue levels (see Figure S2 in the Supplementary Materials) which also included

153 similar questions from the first questionnaire to identify if they experienced any persistent

154 or new symptoms. Please note this questionnaire (Figure S2) has been used to assess

155 fatigue in patients with Chronic Fatigue Syndrome (CFS) and Fibromyalgia (Natelson,
156 2019). To avoid confounding effects from comorbidities, we recruited subjects that were,
157 otherwise, in excellent health conditions prior to hospitalization for COVID-19. For
158 example, 16/47 (34.04%) of our patients were young adults who had no prior record of
159 any comorbidities that could confound the COVID-19 effects. We only had 7/47 (14.89%)
160 subjects with age between 50-54 years (capped at < 55 years as recruitment criteria to
161 avoid aging-related comorbidities), some of whom had reported to have marginal
162 diabetes. The rest (51.07%) in between also did not have any record of comorbidities in
163 the hospital report.

164 *Table 1* summarizes the clinical information from the 47 patients included in the current
165 study. Of these 47, 36.17% (17/47) patients were reported to be 'mild', 8.51% (4/47) to
166 be 'moderate' and 36.17% (17/47) to be 'severe'. Information from the rest of the 19.15%
167 (9/47) was not provided from the hospital because those patients did not give consent to
168 sharing their medical symptoms. Please note, we present percentages as a ratio of
169 affected patients with both the available sample with information ('% Out of Avail.' in *Table*
170 *1*) and the total sample of patients including those patients who did not give consent to
171 publicly share their clinical data ('% Out of Total' in *Table 1*). The percentages of
172 'moderate-severe' patients who were administered medications, e.g., Remdesivir,
173 Dexamethasone, Ceftriaxone, Clexane and other antibiotic regimes are provided in *Table*
174 *1*. On average these 47 patients stayed in the hospital for approximately 11 ± 3.30 [SD]
175 days.

176 *Table 2* summarizes the participant demographics based on age, sex and fatigue. The
177 average age in the HC group was 33.50 ± 9.74 [SD] years and that in the COVID group

178 was 34.63 ± 11.54 [SD] years. The number of males was comparatively higher than
179 females in the HC group 23M vs. 7F, however, the same was true for the COVID group
180 31M vs. 15F. The participants were asked through a questionnaire (see Supplementary
181 Materials, Figure S2), what level of fatigue do they experience during their daily work.
182 Note this 'work' is related to their daily profession and not household chores. They were
183 asked to rate their fatigue levels on a scale of 0 to 5, with 0 representing no fatigue and
184 5 representing the highest fatigue possible. The healthy group underwent the same
185 questionnaire and reported their daily fatigue levels during work. Fatigue scores were
186 successfully obtained from HC ($n = 17$) and COVID ($n = 27$) groups. The mean and
187 standard deviations of fatigue scores in the HC group was 0.65 ± 0.79 [SD] and that of
188 the COVID group was 2.93 ± 1.21 [SD].

189 **Clinical Assessment**

190 The most frequently reported symptoms from the participants (see Supplementary
191 Materials, Figure S1 for questionnaire used) during hospitalization were - fever, cough,
192 body ache, chills, difficulty breathing, bowel irritation, nausea, loss of sense of smell and
193 loss of consciousness. From the day of discharge till the day of scan, we further asked if
194 the participants were experiencing any persistent or new symptoms. Work-related fatigue
195 (86.84%), muscle pain (18.42), lack of sleep (39.47%), lack of attention (36.84%),
196 headache (36.84%), joint pain (50%), memory loss (34.21%), delayed recovery of sense
197 of smell (44.74%) and/or taste (34.21%), bowel irritation (57.89%) and interestingly, hair
198 loss (81.58%) were commonly reported. Please note, most survivors experienced multiple
199 symptoms simultaneously, hence the '%' represents symptoms that overlap within

200 participants. For example, 36.84% of COVID participants reporting with lack of attention
201 also reported a work-related fatigue score > 2.

202

203 **Brain Imaging**

204 **Anatomical MRI** – High-resolution T1-weighted images were acquired on a 3T GE
205 scanner with a 32-channel head coil in 3D imaging mode with a fast BRAVO sequence.
206 The imaging parameters were TI = 450 ms; 244 x 200 matrix; Flip angle = 12 and FOV =
207 256 mm. The subject was placed in a supine position and the whole brain was scanned
208 in the sagittal configuration where 152 slices were collected, and each slice was 1.00 mm
209 thick. The spatial resolution of all the anatomical scans was 1.0 mm x 1.0 mm x 1.0 mm.

210 **Resting-state fMRI** – A gradient echo planar imaging (EPI) was used to obtain 200
211 whole-brain functional volumes. The parameters were: TR = 2000 ms; TE = 30 ms; Flip
212 angle = 90, 38 slices, matrix = 64x64; FOV = 240 x 240 mm²; acquisition voxel size =
213 3.75 x 3.75 x 3 mm³. The participant was requested to stay as still and motionless as
214 possible with eyes fixed to a cross on an overhead screen. Please note, while initially we
215 kept our scanning time limited to collecting 200 time points due to severe pandemic
216 conditions, as conditions eased, we increased our scanning time to collect 400 time points
217 in this ongoing study.

218 **Data Pre-Processing**

219 The data preprocessing was performed primarily using Statistical Parametric Mapping 12
220 (SPM12) toolbox (<http://www.fil.ion.ucl.ac.uk/spm/>) within a MATLAB environment (The
221 MathWorks, Inc., Natick, MA, USA). However, some steps utilized useful tools from FSL

222 (FMRIB Analysis Group, Oxford, UK) and AFNI (<http://afni.nimh.nih.gov/afni>) (Cox, 1996)
223 for housekeeping, visual inspection and quality control purposes. At the beginning, first
224 five time points were excluded from each subject to account for magnetic stabilization.
225 The functional images were motion corrected for head movement using a least squared
226 approach and 6 parameters (rigid body) spatial transformation with respect to the mean
227 image of the scan. The subjects with excessive head motion were identified using
228 framewise displacement (FWD) (Power et al., 2012). Additionally, time frames with high
229 FWD crossing a threshold of 0.5 mm (Power et al., 2012) were identified along with the
230 previous and the next two frames and added as regressors (Yan et al., 2016) during
231 temporal regression of nuisance signals. If more than 50% of the time series data were
232 affected due to regression of high motion frames the participant was removed from the
233 analysis. Moreover, any participant with the maximum framewise translation or rotation
234 exceeding 2 mm was removed from further analysis. Anatomical image from each subject
235 was coregistered to the mean functional image obtained from the motion correction step.
236 T1-weighted image from each subject was segmented into gray matter (GM), white matter
237 (WM), and cerebrospinal fluid (CSF) tissue probability maps and an average template
238 including all participants was generated using DARTEL (Ashburner, 2007). The subject
239 specific tissue maps were non-linearly warped to this template and spatially normalized
240 to the MNI space. These affine transformations were applied to the functional images to
241 normalize all volumes to the MNI space and resampled to isotropic voxel size of 3 mm x
242 3 mm x 3 mm. Time series, from brain compartments with high physiological noise signals
243 such as, CSF and WM was extracted by thresholding the probability maps from the
244 segmentation stage above the 99th percentile, and first 5 principal components were

245 obtained using a COMPCOR based (Behzadi et al., 2007) principal component analysis
246 (PCA) from both tissues. These 10 components along with Friston's 24- parameter model
247 (6 head motion parameters + 6 previous time point motion parameters + 12 corresponding
248 quadratic parameters) (Friston et al., 1996) and time frames with high FWD (> 0.5 mm)
249 were added as regressors in a multiple linear regression model to remove unwanted
250 signals voxel-wise. The residuals from the regression step were then bandpass filtered
251 between 0.01 to 0.1 Hz and finally, spatial smoothing was performed using a Gaussian
252 kernel of 6 mm full width at half maximum (FWHM).

253 **Head Motion Assessment**

254 We performed in-scanner head movement assessment using mean Framewise
255 Displacement (FWD) based on the methods depicted in (Power et al., 2012). A two-tailed
256 two-sample student's t-test revealed no significant differences in mean FWD between the
257 two groups ($t = -1.57$, $p = 0.12$, $\alpha = 0.05$).

258 **ICA and Dual Regression**

259 Group level resting state networks were obtained by applying the 'gica' option of the
260 'melodic' module from FSL toolbox (FMRIB Analysis Group, Oxford, UK). All subjects' 4D
261 functional images after pre-processing were temporally concatenated into a 2D matrix of
262 'space' x 'time' as delineated in (C.F. Beckmann, 2009) and 25 spatial maps were
263 obtained. Resting State Networks (RSNs) were identified by matching ICs with the 1000
264 functional connectome project maps (Biswal et al., 2010) using Dice's coefficient and
265 spatial correlations obtained from AFNI's '3dMatch' program (Taylor & Saad, 2013).
266 Further visual inspection was performed to make sure all network regions aligned with

267 the functional network and ROIs depicted in (Altmann et al., 2015; Shirer et al., 2012).
268 Dual regression (C.F. Beckmann, 2009; Filippini et al., 2009) was performed leveraging
269 the standardized group ICA output from the ‘melodic’ step and applying it directly to the
270 ‘fsl-glm’ module in FSL to obtain subject specific RSN maps. The subject specific network
271 maps were standardized to Z-scores before consequently applying them in statistical
272 analysis to infer group level estimates.

273 **Statistical Analysis**

274 To investigate differences in participant demographics, we performed a two-sample *t-test*
275 on age. Since sex is a categorical variable, we performed a *chi-squared* test to identify
276 any sex related differences between the groups. Since the fatigue scores deviated from
277 normality (*Shapiro-Wilk*, $p < 0.05$), we performed a non-parametric *Wilcoxon-Ranksum*
278 *test* on the fatigue scores to identify group level differences in fatigue scores.

279 To investigate FC differences between COVID and HC groups, we performed an unpaired
280 two sample t-test between standardized subject-specific RSN maps from the two groups.
281 To account for confounding effects that may explain some of the variance in the data,
282 age, sex and a regressor to account for two different scanning lengths were also added
283 as covariates of no interest. Cluster-based thresholding was applied at a height threshold
284 of $p_{unc} < 0.01$, with *family wise error (FWE)* correction at $p_{FWE} < 0.05$ for multiple
285 comparisons. The cluster extent threshold (k_E) obtained from this step was used to
286 threshold and generate corrected statistical maps for the contrasts with significant effects.

287 We further wanted to evaluate if the PRN demonstrates correlation with self-reported
288 fatigue among the COVID individuals. We incorporated a multiple linear regression
289 approach where the FC at each voxel was the response variable (Y), and the self-reported
290 fatigue score was the explanatory variable (X). We also added age and sex as covariates
291 of no interest. Significant clusters were obtained in the same manner as described earlier
292 at the end of the previous paragraph for group level differences in FC. For visual
293 representation of the significant relationship between the two variables, the average FC
294 within the significant cluster was obtained from each subject. These average FC values
295 were then linearly regressed against the fatigue scores and visualized within a scatter
296 plot and a line of best fit with 95% confidence interval. Age and sex were regressed out
297 during the linear regression step. The correlation analysis and the graphical plotting was
298 done using 'inhouse' scripts prepared in RStudio (RStudio, 2021).

299 **Results**

300
301 We will present results on participant demographics first and then group level voxel-wise
302 results will be reported. There was no significant differences in age between the two
303 groups ($p > 0.05$). A *chi-squared* test on sex revealed no significant effects were observed
304 between the two groups ($p > 0.05$). The Wilcoxon-Ranksum test revealed significantly
305 higher fatigue levels in the COVID group compared to the HC group ($T = 1093$, $p = 2.86e-$
306 07).

307 We identified twenty-two large-scale resting state networks (RSNs) (see Figure 1) from
308 the group ICA analysis. Group level statistical analysis was run for five networks of

309 interest using standardized subject specific RSN maps obtained from the dual regression
310 step. Significant differences in FC was observed between the COVID and HC groups in
311 particularly three out of the five networks – the *basal ganglia (BGN)*, *precuneus (PRN)*
312 and *language (LANG)* networks. Figure 2 shows all significant clusters from obtained from
313 the *t*-test and the corresponding group level networks where these alterations occur.

314 Figure 2 A (top row) demonstrates regions with significantly enhanced FC in the COVID-
315 19 group compared to the HC group for the *BGN* network. The FC of the *BGN* network
316 was enhanced within the *Right – Calcarine Cortex (Calc)*, *Cuneus (Cu)* and *Lingual Gyrus*
317 (*LiG*) regions, comprising the *occipital* lobe. Similarly, the COVID survivors also
318 demonstrated enhanced FC of the *PRN* network (Figure 2 B) with regions from the
319 *Parietal Lobe: Bilateral – Superior Parietal Lobule (SPL)* and *Precuneus (PCu)* regions.
320 On the other hand, for the *LANG* network, Figure 2 C shows reduced functional
321 connectivity among COVID participants compared to HCs in several layers of the
322 *cerebellar vermal lobules (CVL) (I-V, VI-VII)*. The cluster peak information including peak
323 *t*-scores and *FWE* corrected exact p-values with relevant anatomical regions from each
324 network have been tabulated for an easy reference in *Table 3*.

325 Figure 3 shows brain regions where a significant negative correlation was observed
326 between FC and self-reported fatigue, from the *PRN* network. The statistic map (Figure
327 3, *left*) shows the cluster where a negative correlation between FC of the *PRN* network
328 and fatigue scores was observed in the *Left – Superior Parietal Lobule (SPL)*, *Superior*
329 *Occipital Gyrus (SOG)*, *Angular Gyrus (AnG)* and *Precuneus (PCu)*. The graph on the
330 right visually portrays this negative relationship (*Spearman's* $\rho = -0.47$, $p = 0.001$, $r^2 =$
331 0.22) between the average FC of this cluster and fatigue scores. The scatter plot (Figure

332 3, *right*) clearly shows that the effects of FC and fatigue are significantly larger in the
333 COVID group (light pink dots higher than cyan dots) compared to HC group. A more
334 intuitive version of this figure can be found within the Supplementary Materials (see Figure
335 S3) where the linear regression line within each group is demonstrated separately to
336 clearly show that the COVID group was more susceptible to fatigue and majorly drove the
337 overall linear trend shown in Figure 3. This can be observed from a significantly stronger
338 correlation between FC and fatigue among survivors ($\rho = -0.72$, $p = 0.00002$, $r^2 = 0.52$)
339 compared to the HC group ($\rho = -0.36$, $p = 0.163$, $r^2 = 0.13$).

340 Discussion

341 The results from this study support our hypothesis that COVID survivors demonstrate
342 altered FC when compared to HCs, even two weeks after discharge from the hospital.
343 Furthermore, the results from the work-related fatigue analysis support the hypothesis
344 that the COVID survivors experience significantly higher fatigue during work and
345 demonstrate more susceptibility to fatigue, with stronger negative correlation of FC and
346 fatigue compared to HCs. Our hypothesis on FC alterations was based on both early
347 case-reports and more recent group level neuroimaging reports of structural and
348 functional brain alterations. Individual case reports were primarily from acutely ill patients
349 using FLAIR (Kandemirli et al., 2020; Kremer, Lersy, Anheim, et al., 2020; Paterson et
350 al., 2020) and Susceptibility Weighted Imaging (SWI) (Conklin et al., 2021), whereas,
351 group level reports, such as those derived from fMRI, include, reduced *default mode* and
352 *salience* connectivity (Fischer et al., 2021) and high prevalence of abnormal time varying
353 and topological organizations between *sensorimotor* and *visual* networks (Fu et al., 2021).

354 In the current context, we report between group FC alterations of three large scale RSNs
355 – *BGN*, *PRN* and *LANG* networks and further show stronger negative correlation between
356 FC in the *PRN* network with self-reported fatigue at work in COVID survivors compared
357 to the HC group.

358 We observed enhanced FC of the *BGN* network in the COVID survivors compared to the
359 HCs within *Calc*, *Cu* and *LiG*. *Calc* and *Cu* are primarily involved in visual processing. Fu
360 and colleagues reported that COVID survivors demonstrated enhanced connectivity
361 between *Cerebellum*, *Sensorimotor* and *Visual* networks, characterizing that they spent
362 abnormally higher time in a specific brain state compared to healthy controls (Fu et al.,
363 2021). A recent study has also suggested *Cu* to be a major hub for mild cognitive
364 impairment in idiopathic REM sleep behavior disorder (iRBD) (Mattioli et al., 2021). *LiG*
365 and weak *insular* coactivation with the *occipital* cortex have been shown to be associated
366 with disrupted salience processing that can lead to loss in motivation in day-to-day tasks
367 (Kim et al., 2018). Interestingly, cortical thickness alterations were also reported in *Calc*
368 and *LiG* regions in non-hospitalized and mildly symptomatic survivors (Crunfli et al.,
369 2021). In our cohort of hospitalized survivors, we expect these alterations to scale up with
370 severity, as severity tends to increase chances of neurological manifestations in
371 hospitalized COVID-19 survivors (Mao et al., 2020). Moreover, the *basal ganglia* are
372 known to be associated with fatigue (Miller et al., 2014), cognitive, emotional and attention
373 processing (Di Martino et al., 2008; van Schouwenburg et al., 2015). The synergy of these
374 studies to our findings indicates possible functional brain associations of commonly
375 observed symptoms in survivors with post-acute sequelae SARS-CoV-2 infection (PASC

376 or Long COVID) lasting many months (Carfi et al., 2020; Garrigues et al., 2020; Logue et
377 al., 2021; Peluso et al., 2021).

378 We observed enhanced FC of the *PRC* network among COVID survivors compared to
379 the HC group. Enhanced FC in this network was observed in the *Bilateral SPL* and *PCu*
380 regions. *PCu* is a constituent of *DMN*, and higher functional connectivity with this region
381 may indicate some compensatory mechanism due to loss in connections in other
382 pathways. Moreover, alterations between *DMN* and *salience* connectivity has been
383 recently reported in a follow-up study from Fischer and colleagues (Fischer et al., 2020),
384 although, initially, a single patient showed no differences in FC of *DMN* when compared
385 to five healthy controls (Fischer et al., 2020). *PRN* network consists of *Precuneus (PCu)*,
386 *Frontal Eye Fields (FEF)* and parts of the *Superior Parietal Lobule (SPL)*. *SPL* is a
387 constituent of the *posterior parietal cortex (PPC)* which has been shown to have functional
388 association with altered *anterior insula* connectivity in CFS (Wortinger et al., 2017).
389 Moreover, these brain regions are also known to be involved in attention processing,
390 therefore, enhanced FC in these regions may indicate possible compensatory
391 mechanisms of attention related symptoms that recovering patients may experience. This
392 is significant, because about 37% of the COVID survivors in our study reported lack of
393 attention and all these 37% of the participants also reported a work-related fatigue score
394 of 2 or higher on a scale of 5. Therefore, further investigations are necessary to
395 understand these processes better, especially, from a clinical perspective.

396 We also observed reduced FC of the *LANG* network within several layers of the
397 *Cerebellar Vermal Lobules* among COVID participants when compared to HCs. These
398 lobules have been suggested to be involved in cognition and emotion processing (Park

399 et al., 2018). Interestingly, structural alterations have also been reported in these layers
400 among COVID survivors. A case report of a 47-year-old male described hyperintense
401 *bilateral cerebellar hemisphere* and *cerebellar vermis*, which was also the first reported
402 case of acute cerebellitis in COVID-19 (Fadakar et al., 2020). Another case of cerebellitis
403 was also reported recently, adding on to the wide range of neurological disturbances in
404 the CNS (Malayala et al., 2021). Moreover, approximately 45% of the survivors in the
405 study experienced loss/reduction of sense of smell or hyposmia. Activation in the
406 *cerebellum*, specifically in the *vermal lobules*, through olfactory stimulation has been
407 shown both in humans (Ferdon & Murphy, 2003) and animals (García et al., 2015).
408 Reduced FC within *cerebellar vermal layers* may indicate connectivity deficits, as a result
409 of olfactory dysfunction.

410 We observed FC alterations in three out of five networks of interest. The neuro-invasion
411 of the coronavirus can spread and sustain throughout the brain, causing pathologies
412 several months after the initial infection (Daniel et al., 2022), possibly leading to
413 development of PASC. (Daniel et al., 2022) also found traces of the virus in brain tissue
414 biopsies even from mild and asymptomatic patients. Therefore, perhaps with time, more
415 and more structural and functional networks in these survivors will be affected during the
416 transition phase to PASC. With the availability of more sample data and a follow-up
417 design, perhaps all brain networks can be investigated for a more comprehensive
418 understanding of the brain pathologies systematically. RS-fMRI can be quite useful in this
419 regard because it facilitates the investigation of multiple brain networks across the whole
420 brain (Damoiseaux et al., 2006; Raichle & Mintun, 2006; Shulman et al., 2004). The
421 results also suggest a possible link between structural and functional abnormalities in

422 COVID survivors since the FC alterations were observed in regions that align with
423 anatomical regions exhibiting hyperintensities, particularly, in the *basal ganglia* (Paterson
424 et al., 2020), *parietal* and *occipital* lobes (Kandemirli et al., 2020) as well as in *cerebellar*
425 regions (Kremer, Lersy, de Sèze, et al., 2020). We do not know how the functional
426 abnormalities in these survivors relate to PASC, however, cerebrovascular injuries and
427 inflammatory processes may play an important role in determining whether a patient
428 returns to normal health or continues ill with PASC. Neurological damage and
429 abnormalities found in cerebral arteries in several acute patients across various centers
430 (Gulko et al., 2020), can imply different levels of cerebral blood flow alterations in PASC
431 and not-PASC survivors. Thus, it is possible that functional changes will be observed
432 between PASC and not-PASC COVID survivors in future studies.

433 Based on recent literature on PASC patients, fatigue has been the most frequently
434 reported symptom (Logue et al., 2021; Peluso et al., 2021; Tabacof et al., 2020). In the
435 current study, we also observed that fatigue during work was the highest reported
436 symptom (86.84%) among COVID survivors 2 weeks after hospital discharge. We
437 observed higher fatigue levels among COVID survivors when compared to healthy
438 controls ($p < 0.001$). We further evaluated linear relationship between FC of the *PRC*
439 network and self-reported fatigue at work across both COVID and HC participants. We
440 observed a significant negative correlation of FC with fatigue within the *Left SPL*, *SOG*,
441 *AnG* and *PCu*, i.e., brain regions primarily belonging to the *parietal* lobe (see *Table 4* for
442 cluster information). Interestingly, our recent investigation using the same group of
443 survivors revealed stronger positive correlation between GMV and self-reported fatigue
444 within the *precuneus* and *SPL* regions, when compared to HCs (Hafiz et al., 2022). This

445 provides supporting evidence to our hypothesis that COVID survivors also demonstrate
446 stronger correlation between FC and fatigue in the *PRC* network, based on our previous
447 observation on GMV and fatigue relationship in these regions. Moreover, structural
448 atrophy in the *parietal lobe* has been shown to be associated with fatigue among multiple
449 sclerosis (MS) patients (Calabrese et al., 2010; Pellicano et al., 2010). An RS-fMRI study
450 involving CFS patients, used ICA to reveal loss of intrinsic connectivity in the *parietal lobe*
451 (Gay et al., 2016). Therefore, the fact that lower FC in the *parietal lobe* correlates more
452 negatively to higher fatigue scores among COVID survivors, can be clinically relevant
453 because it matches both structural and functional relationships with fatigue in other
454 neurological disorders such as MS and CFS. To the best of our knowledge, this is the first
455 study to show work-related fatigue correlates of FC among recovering patients 2 weeks
456 after hospital discharge. Therefore, future studies are necessary to evaluate this highly
457 prevalent symptom further in the surviving cohorts.

458

459 **Limitations**

460 Despite our efforts to show group level effects that reflect individual and group level
461 reports in the recent literature, our study still maintains a cross-sectional design. In cases
462 like this, a better approach for the future would be to use follow up designs (Fu et al.,
463 2021; Lu et al., 2020; Tu et al., 2021) or possibly a longitudinal design where patients
464 could be observed both before and after the pandemic like the one using the UK-biobank
465 (Douaud et al., 2021). Our effort here, was to show group level effects at an early stage
466 of recovery (2 weeks after hospital discharge) and determine the relation between work-

467 related fatigue and FC of RSNs. We believe the results from this study will help
468 understanding the recovery stage brain alterations and how they might drive fatigue-
469 related symptoms among COVID survivors.

470

471

472 **Author Credit Statement**

473

474 **Rakibul Hafiz:** Methodology, Software, Formal Analysis, Data Curation, Writing –

475 Original Draft, Review and Editing.

476 **Tapan K. Gandhi:** Conceptualization, Investigation, Resources, Supervision, Writing –

477 Review and Editing.

478 **Sapna Mishra:** Investigation, Resources, Data Curation, Writing – Review and Editing.

479 **Alok Prasad:** Writing – Review and Editing.

480 **Vidur Mahajan:** Writing – Review and Editing.

481 **Xin Di:** Methodology, Writing – Review and Editing.

482 **Benjamin H. Natelson:** Writing – Review and Editing.

483 **Bharat Biswal:** Conceptualization, Resources, Project Administration, Supervision,

484 Writing – Review and Editing.

485

486 **Acknowledgements**

487 This study was supported by NIH grants: R01AT009829 and R01MH131335 and MeitY

488 (Government of India) under Grant No: 4(16)/2019-ITEA

489

490

492 References

- 493 (WHO), W. H. O. (2020, 10/21/2021, 4:46pm CET). *WHO Coronavirus Disease (COVID-19)*
494 *Dashboard*. Retrieved 10/21/2021 from <https://covid19.who.int/table>
- 495 Altmann, A., Ng, B., Landau, S. M., Jagust, W. J., & Greicius, M. D. (2015). Regional brain
496 hypometabolism is unrelated to regional amyloid plaque burden. *Brain*, *138*(Pt 12),
497 3734-3746. <https://doi.org/10.1093/brain/awv278>
- 498 Amunts, K., Kedo, O., Kindler, M., Pieperhoff, P., Mohlberg, H., Shah, N. J., Habel, U.,
499 Schneider, F., & Zilles, K. (2005). Cytoarchitectonic mapping of the human amygdala,
500 hippocampal region and entorhinal cortex: intersubject variability and probability
501 maps. *Anatomy and Embryology*, *210*(5), 343-352. [https://doi.org/10.1007/s00429-](https://doi.org/10.1007/s00429-005-0025-5)
502 [005-0025-5](https://doi.org/10.1007/s00429-005-0025-5)
- 503 Ashburner, J. (2007). A fast diffeomorphic image registration algorithm. *Neuroimage*, *38*(1),
504 95-113. <https://doi.org/10.1016/j.neuroimage.2007.07.007>
- 505 Behzadi, Y., Restom, K., Liao, J., & Liu, T. T. (2007). A component based noise correction
506 method (CompCor) for BOLD and perfusion based fMRI. *Neuroimage*, *37*(1), 90-101.
507 <https://doi.org/10.1016/j.neuroimage.2007.04.042>
- 508 Benedetti, F., Palladini, M., Paolini, M., Melloni, E., Vai, B., De Lorenzo, R., Furlan, R., Rovere-
509 Querini, P., Falini, A., & Mazza, M. G. (2021). Brain correlates of depression, post-
510 traumatic distress, and inflammatory biomarkers in COVID-19 survivors: A
511 multimodal magnetic resonance imaging study. *Brain, behavior, & immunity - health*,
512 *18*, 100387-100387. <https://doi.org/10.1016/j.bbih.2021.100387>
- 513 Biswal, B., Yetkin, F. Z., Haughton, V. M., & Hyde, J. S. (1995). Functional connectivity in the
514 motor cortex of resting human brain using echo-planar MRI. *Magn Reson Med*, *34*(4),
515 537-541.
- 516 Biswal, B. B., Mennes, M., Zuo, X.-N., Gohel, S., Kelly, C., Smith, S. M., Beckmann, C. F.,
517 Adelstein, J. S., Buckner, R. L., Colcombe, S., Dogonowski, A.-M., Ernst, M., Fair, D.,
518 Hampson, M., Hoptman, M. J., Hyde, J. S., Kiviniemi, V. J., Kötter, R., Li, S.-J., . . . Milham,
519 M. P. (2010). Toward discovery science of human brain function. *Proceedings of the*
520 *National Academy of Sciences*, *107*(10), 4734-4739.
521 <https://doi.org/10.1073/pnas.0911855107>
- 522 C.F. Beckmann, C. E. M., N. Filippini, and S.M. Smith. (2009). Group comparison of resting-
523 state FMRI data using multi-subject ICA and dual regression. *OHBM*.
- 524 Calabrese, M., Rinaldi, F., Grossi, P., Mattisi, I., Bernardi, V., Favaretto, A., Perini, P., & Gallo,
525 P. (2010). Basal ganglia and frontal/parietal cortical atrophy is associated with
526 fatigue in relapsing-remitting multiple sclerosis. *Mult Scler*, *16*(10), 1220-1228.
527 <https://doi.org/10.1177/1352458510376405>
- 528 Carfi, A., Bernabei, R., Landi, F., & Gemelli Against, C.-P.-A. C. S. G. (2020). Persistent
529 Symptoms in Patients After Acute COVID-19. *JAMA*, *324*(6), 603-605.
530 <https://doi.org/10.1001/jama.2020.12603>
- 531 Cavanna, A. E., & Trimble, M. R. (2006). The precuneus: a review of its functional anatomy
532 and behavioural correlates. *Brain*, *129*(3), 564-583.
533 <https://doi.org/10.1093/brain/awl004>
- 534 Cole, D. M., Smith, S. M., & Beckmann, C. F. (2010). Advances and pitfalls in the analysis and
535 interpretation of resting-state FMRI data. *Front Syst Neurosci*, *4*, 8.
536 <https://doi.org/10.3389/fnsys.2010.00008>

- 537 Conklin, J., Frosch, M. P., Mukerji, S. S., Rapalino, O., Maher, M. D., Schaefer, P. W., Lev, M. H.,
538 Gonzalez, R. G., Das, S., Champion, S. N., Magdamo, C., Sen, P., Harrold, G. K., Alabsi, H.,
539 Normandin, E., Shaw, B., Lemieux, J. E., Sabeti, P. C., Branda, J. A., . . . Edlow, B. L.
540 (2021). Susceptibility-weighted imaging reveals cerebral microvascular injury in
541 severe COVID-19. *Journal of the Neurological Sciences*, 421, 117308-117308.
542 <https://doi.org/10.1016/j.jns.2021.117308>
- 543 Cox, R. W. (1996). AFNI: software for analysis and visualization of functional magnetic
544 resonance neuroimages. *Comput Biomed Res*, 29(3), 162-173.
- 545 Crunfli, F., Carregari, V. C., Veras, F. P., Vendramini, P. H., Valença, A. G. F., Antunes, A. S. L.
546 M., Brandão-Teles, C., Zucoli, G. d. S., Reis-de-Oliveira, G., Silva-Costa, L. C., Saia-
547 Cereda, V. M., Smith, B. J., Codo, A. C., de Souza, G. F., Muraro, S. P., Parise, P. L.,
548 Toledo-Teixeira, D. A., de Castro, Í. M. S., Melo, B. M. S., . . . Martins-de-Souza, D.
549 (2021). SARS-CoV-2 infects brain astrocytes of COVID-19 patients and impairs
550 neuronal viability. *medRxiv*, 2020.2010.2009.20207464.
551 <https://doi.org/10.1101/2020.10.09.20207464>
- 552 Damoiseaux, J. S., Rombouts, S. A., Barkhof, F., Scheltens, P., Stam, C. J., Smith, S. M., &
553 Beckmann, C. F. (2006). Consistent resting-state networks across healthy subjects.
554 *Proc Natl Acad Sci U S A*, 103(37), 13848-13853.
555 <https://doi.org/10.1073/pnas.0601417103>
- 556 Daniel, C., Sydney, S., Sabrina, R., Alison, G., Joon-Yong, C., Manmeet, S., Claude Kwe, Y.,
557 Clayton, W., James, D., Kris, Y., Sung Hee, K., Andrew, P., Peter, B., Martha, Q., Stefania,
558 P., Madeleine, P., Vincent, M., Frida, B., Marcos, R.-B., . . . David, K. (2022). SARS-CoV-
559 2 infection and persistence throughout the human body and brain. *Nature Portfolio*.
560 <https://doi.org/10.21203/rs.3.rs-1139035/v1>
- 561 De Luca, M., Beckmann, C. F., De Stefano, N., Matthews, P. M., & Smith, S. M. (2006). fMRI
562 resting state networks define distinct modes of long-distance interactions in the
563 human brain. *Neuroimage*, 29(4), 1359-1367.
564 <https://doi.org/10.1016/j.neuroimage.2005.08.035>
- 565 Di Martino, A., Scheres, A., Margulies, D. S., Kelly, A. M., Uddin, L. Q., Shehzad, Z., Biswal, B.,
566 Walters, J. R., Castellanos, F. X., & Milham, M. P. (2008). Functional connectivity of
567 human striatum: a resting state FMRI study. *Cereb Cortex*, 18(12), 2735-2747.
568 <https://doi.org/10.1093/cercor/bhn041>
- 569 Douaud, G., Lee, S., Alfaro-Almagro, F., Arthofer, C., Wang, C., Lange, F., Andersson, J. L. R.,
570 Griffanti, L., Duff, E., Jbabdi, S., Taschler, B., Winkler, A., Nichols, T. E., Collins, R.,
571 Matthews, P. M., Allen, N., Miller, K. L., & Smith, S. M. (2021). Brain imaging before
572 and after COVID-19 in UK Biobank. *medRxiv*.
573 <https://doi.org/10.1101/2021.06.11.21258690>
- 574 Duan, K., Premi, E., Pilotto, A., Cristillo, V., Benussi, A., Libri, I., Giunta, M., Bockholt, H. J., Liu,
575 J., Campora, R., Pezzini, A., Gasparotti, R., Magoni, M., Padovani, A., & Calhoun, V. D.
576 (2021). Alterations of frontal-temporal gray matter volume associate with clinical
577 measures of older adults with COVID-19. *Neurobiol Stress*, 14, 100326.
578 <https://doi.org/10.1016/j.ynstr.2021.100326>
- 579 Esposito, F., Cirillo, M., De Micco, R., Caiazzo, G., Siciliano, M., Russo, A. G., Monari, C.,
580 Coppola, N., Tedeschi, G., & Tessitore, A. (2022). Olfactory loss and brain
581 connectivity after COVID-19 [<https://doi.org/10.1002/hbm.25741>]. *Hum Brain*
582 *Mapp*, n/a(n/a). <https://doi.org/https://doi.org/10.1002/hbm.25741>

- 583 Fadakar, N., Ghaemmaghami, S., Masoompour, S. M., Shirazi Yeganeh, B., Akbari, A.,
584 Hooshmandi, S., & Ostovan, V. R. (2020). A First Case of Acute Cerebellitis Associated
585 with Coronavirus Disease (COVID-19): a Case Report and Literature Review.
586 *Cerebellum (London, England)*, 19(6), 911-914. [https://doi.org/10.1007/s12311-](https://doi.org/10.1007/s12311-020-01177-9)
587 [020-01177-9](https://doi.org/10.1007/s12311-020-01177-9)
- 588 Favaro, A., Santonastaso, P., Manara, R., Bosello, R., Bommarito, G., Tenconi, E., & Di Salle, F.
589 (2012). Disruption of visuospatial and somatosensory functional connectivity in
590 anorexia nervosa. *Biol Psychiatry*, 72(10), 864-870.
591 <https://doi.org/10.1016/j.biopsych.2012.04.025>
- 592 Ferdon, S., & Murphy, C. (2003). The cerebellum and olfaction in the aging brain: a
593 functional magnetic resonance imaging study. *Neuroimage*, 20(1), 12-21.
594 [https://doi.org/https://doi.org/10.1016/S1053-8119\(03\)00276-3](https://doi.org/10.1016/S1053-8119(03)00276-3)
- 595 Filippini, N., MacIntosh, B. J., Hough, M. G., Goodwin, G. M., Frisoni, G. B., Smith, S. M.,
596 Matthews, P. M., Beckmann, C. F., & Mackay, C. E. (2009). Distinct patterns of brain
597 activity in young carriers of the APOE-epsilon4 allele. *Proc Natl Acad Sci U S A*,
598 106(17), 7209-7214. <https://doi.org/10.1073/pnas.0811879106>
- 599 Fischer, D., Snider, S. B., Barra, M. E., Sanders, W. R., Rapalino, O., Schaefer, P., Foulkes, A. S.,
600 Bodien, Y. G., & Edlow, B. L. (2021). Disorders of Consciousness Associated With
601 COVID-19: A Prospective, Multimodal Study of Recovery and Brain Connectivity.
602 *Neurology*. <https://doi.org/10.1212/wnl.0000000000013067>
- 603 Fischer, D., Threlkeld, Z. D., Bodien, Y. G., Kirsch, J. E., Huang, S. Y., Schaefer, P. W., Rapalino,
604 O., Hochberg, L. R., Rosen, B. R., & Edlow, B. L. (2020). Intact Brain Network Function
605 in an Unresponsive Patient with COVID-19. *Annals of neurology*, 88(4), 851-854.
606 <https://doi.org/10.1002/ana.25838>
- 607 Fox, M. D., Snyder, A. Z., Vincent, J. L., Corbetta, M., Van Essen, D. C., & Raichle, M. E. (2005).
608 The human brain is intrinsically organized into dynamic, anticorrelated functional
609 networks. *Proc Natl Acad Sci U S A*, 102(27), 9673-9678.
610 <https://doi.org/10.1073/pnas.0504136102>
- 611 Fox, M. D., Snyder, A. Z., Zacks, J. M., & Raichle, M. E. (2006). Coherent spontaneous activity
612 accounts for trial-to-trial variability in human evoked brain responses. *Nat Neurosci*,
613 9(1), 23-25. <https://doi.org/10.1038/nn1616>
- 614 Freton, M., Lemogne, C., Bergouignan, L., Delaveau, P., Lehericy, S., & Fossati, P. (2014). The
615 eye of the self: precuneus volume and visual perspective during autobiographical
616 memory retrieval. *Brain Struct Funct*, 219(3), 959-968.
617 <https://doi.org/10.1007/s00429-013-0546-2>
- 618 Friston, K. J. (1994). Functional and effective connectivity in neuroimaging: a synthesis.
619 *Hum Brain Mapp*, 2(1-2), 56-78.
- 620 Friston, K. J., Frith, C. D., Liddle, P. F., & Frackowiak, R. S. (1993). Functional connectivity:
621 the principal-component analysis of large (PET) data sets. *Journal of Cerebral Blood*
622 *Flow & Metabolism*, 13(1), 5-14.
- 623 Friston, K. J., Williams, S., Howard, R., Frackowiak, R. S., & Turner, R. (1996). Movement-
624 related effects in fMRI time-series. *Magn Reson Med*, 35(3), 346-355.
- 625 Fu, Z., Tu, Y., Calhoun, V. D., Zhang, Y., Zhao, Q., Chen, J., Meng, Q., Lu, Z., & Hu, L. (2021).
626 Dynamic functional network connectivity associated with post-traumatic stress
627 symptoms in COVID-19 survivors. *Neurobiology of Stress*, 15, 100377.
628 [https://doi.org/https://doi.org/10.1016/j.ynstr.2021.100377](https://doi.org/10.1016/j.ynstr.2021.100377)

- 629 García, L. I., García-Bañuelos, P., Aranda-Abreu, G. E., Herrera-Meza, G., Coria-Avila, G. A., &
630 Manzo, J. (2015). Activation of the cerebellum by olfactory stimulation in sexually
631 naive male rats. *Neurología (English Edition)*, 30(5), 264-269.
632 <https://doi.org/https://doi.org/10.1016/j.nrleng.2014.02.004>
- 633 Garrigues, E., Janvier, P., Kherabi, Y., Le Bot, A., Hamon, A., Gouze, H., Doucet, L., Berkani, S.,
634 Oliosi, E., Mallart, E., Corre, F., Zarrouk, V., Moyer, J. D., Galy, A., Honsel, V., Fantin, B.,
635 & Nguyen, Y. (2020). Post-discharge persistent symptoms and health-related quality
636 of life after hospitalization for COVID-19. *J Infect*, 81(6), e4-e6.
637 <https://doi.org/10.1016/j.jinf.2020.08.029>
- 638 Gay, C. W., Robinson, M. E., Lai, S., O'Shea, A., Craggs, J. G., Price, D. D., & Staud, R. (2016).
639 Abnormal Resting-State Functional Connectivity in Patients with Chronic Fatigue
640 Syndrome: Results of Seed and Data-Driven Analyses. *Brain Connect*, 6(1), 48-56.
641 <https://doi.org/10.1089/brain.2015.0366>
- 642 Greicius, M. D., Krasnow, B., Reiss, A. L., & Menon, V. (2003). Functional connectivity in the
643 resting brain: a network analysis of the default mode hypothesis. *Proc Natl Acad Sci*
644 *U S A*, 100(1), 253-258. <https://doi.org/10.1073/pnas.0135058100>
- 645 Gulko, E., Oleksk, M. L., Gomes, W., Ali, S., Mehta, H., Overby, P., Al-Mufti, F., & Rozenshtein,
646 A. (2020). MRI Brain Findings in 126 Patients with COVID-19: Initial Observations
647 from a Descriptive Literature Review. *American Journal of Neuroradiology*.
648 <https://doi.org/10.3174/ajnr.A6805>
- 649 Hafiz, R., Gandhi, T. K., Mishra, S., Prasad, A., Mahajan, V., Di, X., Natelson, B. H., & Biswal, B.
650 B. (2022). Higher limbic and basal ganglia volumes in surviving COVID-negative
651 patients and the relations to fatigue. *Neuroimage: Reports*, 2(2), 100095.
652 <https://doi.org/https://doi.org/10.1016/j.ynirp.2022.100095>
- 653 Horwitz, B. (2003). The elusive concept of brain connectivity. *Neuroimage*, 19(2), 466-470.
654 [https://doi.org/https://doi.org/10.1016/S1053-8119\(03\)00112-5](https://doi.org/https://doi.org/10.1016/S1053-8119(03)00112-5)
- 655 Ismail, I. I., & Gad, K. A. (2021). Absent Blood Oxygen Level-Dependent Functional Magnetic
656 Resonance Imaging Activation of the Orbitofrontal Cortex in a Patient With
657 Persistent Cacosmia and Cacogeusia After COVID-19 Infection. *JAMA Neurology*.
658 <https://doi.org/10.1001/jamaneurol.2021.0009>
- 659 Kalcher, K., Huf, W., Boubela, R. N., Filzmoser, P., Pezawas, L., Biswal, B., Kasper, S., Moser,
660 E., & Windischberger, C. (2012). Fully exploratory network independent component
661 analysis of the 1000 functional connectomes database. *Front Hum Neurosci*, 6, 301.
662 <https://doi.org/10.3389/fnhum.2012.00301>
- 663 Kandemirli, S. G., Dogan, L., Sarikaya, Z. T., Kara, S., Akinci, C., Kaya, D., Kaya, Y., Yildirim, D.,
664 Tuzuner, F., Yildirim, M. S., Ozluk, E., Gucyetmez, B., Karaarslan, E., Koyluoglu, I.,
665 Demirel Kaya, H. S., Mammadov, O., Kisa Ozdemir, I., Afsar, N., Citci Yalcinkaya, B., . . .
666 Kocer, N. (2020). Brain MRI Findings in Patients in the Intensive Care Unit with
667 COVID-19 Infection. *Radiology*, 297(1), E232-e235.
668 <https://doi.org/10.1148/radiol.2020201697>
- 669 Kang, L., Zhang, A., Sun, N., Liu, P., Yang, C., Li, G., Liu, Z., Wang, Y., & Zhang, K. (2018).
670 Functional connectivity between the thalamus and the primary somatosensory
671 cortex in major depressive disorder: a resting-state fMRI study. *BMC Psychiatry*,
672 18(1), 339. <https://doi.org/10.1186/s12888-018-1913-6>
- 673 Keller, E., Brandi, G., Winklhofer, S., Imbach, L. L., Kirschenbaum, D., Frontzek, K., Steiger, P.,
674 Dietler, S., Haeberlin, M., Willms, J., Porta, F., Waeckerlin, A., Huber, M., Abela, I. A.,

- 675 Lutterotti, A., Stippich, C., Globas, C., Varga, Z., & Jelcic, I. (2020). Large and Small
676 Cerebral Vessel Involvement in Severe COVID-19: Detailed Clinical Workup of a Case
677 Series. *Stroke*, 51(12), 3719-3722. <https://doi.org/10.1161/strokeaha.120.031224>
- 678 Kim, B. H., Shin, Y. B., Kyeong, S., Lee, S. K., & Kim, J. J. (2018). Disrupted salience processing
679 involved in motivational deficits for real-life activities in patients with
680 schizophrenia. *Schizophr Res*, 197, 407-413.
681 <https://doi.org/10.1016/j.schres.2018.01.019>
- 682 Kremer, S., Lersy, F., Anheim, M., Merdji, H., Schenck, M., Oesterlé, H., Bolognini, F., Messie, J.,
683 Khalil, A., Gaudemer, A., Carré, S., Alleg, M., Lecocq, C., Schmitt, E., Anxionnat, R., Zhu,
684 F., Jager, L., Nesser, P., Mba, Y. T., . . . Cotton, F. (2020). Neurologic and neuroimaging
685 findings in patients with COVID-19: A retrospective multicenter study. *Neurology*,
686 95(13), e1868-e1882. <https://doi.org/10.1212/wnl.0000000000010112>
- 687 Kremer, S., Lersy, F., de Sèze, J., Ferré, J. C., Maamar, A., Carsin-Nicol, B., Collange, O.,
688 Bonneville, F., Adam, G., Martin-Blondel, G., Rafiq, M., Geeraerts, T., Delamarre, L.,
689 Grand, S., & Krainik, A. (2020). Brain MRI Findings in Severe COVID-19: A
690 Retrospective Observational Study. *Radiology*, 297(2), E242-e251.
691 <https://doi.org/10.1148/radiol.2020202222>
- 692 Laurendon, T., Radulesco, T., Mugnier, J., Gérault, M., Chagnaud, C., El Ahmadi, A.-A., &
693 Varoquaux, A. (2020). Bilateral transient olfactory bulb edema during COVID-19-
694 related anosmia. *Neurology*, 95(5), 224-225.
695 <https://doi.org/10.1212/wnl.0000000000009850>
- 696 Lavagnino, L., Amianto, F., D'Agata, F., Huang, Z., Mortara, P., Abbate-Daga, G., Marzola, E.,
697 Spalatro, A., Fassino, S., & Northoff, G. (2014). Reduced resting-state functional
698 connectivity of the somatosensory cortex predicts psychopathological symptoms in
699 women with bulimia nervosa. *Frontiers in Behavioral Neuroscience*, 8, 270-270.
700 <https://doi.org/10.3389/fnbeh.2014.00270>
- 701 Liu, P., Yang, W., Zhuang, K., Wei, D., Yu, R., Huang, X., & Qiu, J. (2021). The functional
702 connectome predicts feeling of stress on regular days and during the COVID-19
703 pandemic. *Neurobiol Stress*, 14, 100285.
704 <https://doi.org/10.1016/j.ynstr.2020.100285>
- 705 Logue, J. K., Franko, N. M., McCulloch, D. J., McDonald, D., Magedson, A., Wolf, C. R., & Chu, H.
706 Y. (2021). Sequelae in Adults at 6 Months After COVID-19 Infection. *JAMA Netw*
707 *Open*, 4(2), e210830. <https://doi.org/10.1001/jamanetworkopen.2021.0830>
- 708 Lu, Y., Li, X., Geng, D., Mei, N., Wu, P.-Y., Huang, C.-C., Jia, T., Zhao, Y., Wang, D., Xiao, A., & Yin,
709 B. (2020). Cerebral Micro-Structural Changes in COVID-19 Patients – An
710 MRI-based 3-month Follow-up Study. *EclinicalMedicine*, 25.
711 <https://doi.org/10.1016/j.eclinm.2020.100484>
- 712 Malayala, S. V., Jaidev, P., Vanaparthi, R., & Jolly, T. S. (2021). Acute COVID-19 Cerebellitis: A
713 Rare Neurological Manifestation of COVID-19 Infection. *Cureus*, 13(10), e18505-
714 e18505. <https://doi.org/10.7759/cureus.18505>
- 715 Mao, L., Jin, H., Wang, M., Hu, Y., Chen, S., He, Q., Chang, J., Hong, C., Zhou, Y., Wang, D., Miao,
716 X., Li, Y., & Hu, B. (2020). Neurologic Manifestations of Hospitalized Patients With
717 Coronavirus Disease 2019 in Wuhan, China. *JAMA Neurology*, 77(6), 683-690.
718 <https://doi.org/10.1001/jamaneurol.2020.1127>
- 719 Matsuda, K., Park, C. H., Sunden, Y., Kimura, T., Ochiai, K., Kida, H., & Umemura, T. (2004).
720 The vagus nerve is one route of transneural invasion for intranasally inoculated

- 721 influenza a virus in mice. *Vet Pathol*, 41(2), 101-107.
722 <https://doi.org/10.1354/vp.41-2-101>
- 723 Mattioli, P., Pardini, M., Famà, F., Girtler, N., Brugnolo, A., Orso, B., Meli, R., Filippi, L.,
724 Grisanti, S., Massa, F., Bauckneht, M., Miceli, A., Terzaghi, M., Morbelli, S., Nobili, F., &
725 Arnaldi, D. (2021). Cuneus/precuneus as a central hub for brain functional
726 connectivity of mild cognitive impairment in idiopathic REM sleep behavior
727 patients. *Eur J Nucl Med Mol Imaging*, 48(9), 2834-2845.
728 <https://doi.org/10.1007/s00259-021-05205-6>
- 729 McCray, P. B., Jr., Pewe, L., Wohlford-Lenane, C., Hickey, M., Manzel, L., Shi, L., Netland, J., Jia,
730 H. P., Halabi, C., Sigmund, C. D., Meyerholz, D. K., Kirby, P., Look, D. C., & Perlman, S.
731 (2007). Lethal infection of K18-hACE2 mice infected with severe acute respiratory
732 syndrome coronavirus. *J Virol*, 81(2), 813-821. [https://doi.org/10.1128/jvi.02012-](https://doi.org/10.1128/jvi.02012-06)
733 [06](https://doi.org/10.1128/jvi.02012-06)
- 734 McKeown, M. J., Makeig, S., Brown, G. G., Jung, T. P., Kindermann, S. S., Bell, A. J., & Sejnowski,
735 T. J. (1998). Analysis of fMRI data by blind separation into independent spatial
736 components. *Hum Brain Mapp*, 6(3), 160-188. [https://doi.org/10.1002/\(SICI\)1097-](https://doi.org/10.1002/(SICI)1097-0193(1998)6:3<#x0003c;160::AID-HBM5#x0003e;3.0.CO;2-1)
737 [0193\(1998\)6:3<#x0003c;160::AID-HBM5#x0003e;3.0.CO;2-1](https://doi.org/10.1002/(SICI)1097-0193(1998)6:3<#x0003c;160::AID-HBM5#x0003e;3.0.CO;2-1)
- 738 Meier, T. B., Wildenberg, J. C., Liu, J., Chen, J., Calhoun, V. D., Biswal, B. B., Meyerand, M. E.,
739 Birn, R. M., & Prabhakaran, V. (2012). Parallel ICA identifies sub-components of
740 resting state networks that covary with behavioral indices. *Front Hum Neurosci*, 6,
741 281. <https://doi.org/10.3389/fnhum.2012.00281>
- 742 Miller, A. H., Jones, J. F., Drake, D. F., Tian, H., Unger, E. R., & Pagnoni, G. (2014). Decreased
743 basal ganglia activation in subjects with chronic fatigue syndrome: association with
744 symptoms of fatigue. *PLoS One*, 9(5), e98156.
745 <https://doi.org/10.1371/journal.pone.0098156>
- 746 Natelson, B. H. (2019). Myalgic Encephalomyelitis/Chronic Fatigue Syndrome and
747 Fibromyalgia: Definitions, Similarities, and Differences. *Clinical Therapeutics*, 41(4),
748 612-618. <https://doi.org/https://doi.org/10.1016/j.clinthera.2018.12.016>
- 749 Nicholson, P., Alshafai, L., & Krings, T. (2020). Neuroimaging Findings in Patients with
750 COVID-19. *American Journal of Neuroradiology*, 41(8), 1380-1383.
751 <https://doi.org/10.3174/ajnr.A6630>
- 752 Niesen, M., Trotta, N., Noel, A., Coolen, T., Fayad, G., Leurkin-Sterk, G., Delpierre, I., Henrard,
753 S., Sadeghi, N., Goffard, J.-C., Goldman, S., & De Tiège, X. (2021). Structural and
754 metabolic brain abnormalities in COVID-19 patients with sudden loss of smell.
755 *European journal of nuclear medicine and molecular imaging*, 48(6), 1890-1901.
756 <https://doi.org/10.1007/s00259-020-05154-6>
- 757 Ogawa, S., Lee, T. M., Kay, A. R., & Tank, D. W. (1990). Brain magnetic resonance imaging
758 with contrast dependent on blood oxygenation. *Proc Natl Acad Sci U S A*, 87(24),
759 9868-9872. <https://doi.org/10.1073/pnas.87.24.9868>
- 760 Park, I. S., Lee, N. J., & Rhyu, I. J. (2018). Roles of the Declive, Folium, and Tuber Cerebellar
761 Vermian Lobules in Sportspeople. *Journal of clinical neurology (Seoul, Korea)*, 14(1),
762 1-7. <https://doi.org/10.3988/jcn.2018.14.1.1>
- 763 Paterson, R. W., Brown, R. L., Benjamin, L., Nortley, R., Wiethoff, S., Bharucha, T., Jayaseelan,
764 D. L., Kumar, G., Raftopoulos, R. E., Zambreanu, L., Vivekanandam, V., Khoo, A.,
765 Gerald, R., Chinthapalli, K., Boyd, E., Tuzlali, H., Price, G., Christofi, G., Morrow, J., . . .
766 Zandi, M. S. (2020). The emerging spectrum of COVID-19 neurology: clinical,

- 767 radiological and laboratory findings. *Brain*, 143(10), 3104-3120.
768 <https://doi.org/10.1093/brain/awaa240>
- 769 Pellicano, C., Gallo, A., Li, X., Ikonomidou, V. N., Evangelou, I. E., Ohayon, J. M., Stern, S. K.,
770 Ehrmantraut, M., Cantor, F., McFarland, H. F., & Bagnato, F. (2010). Relationship of
771 Cortical Atrophy to Fatigue in Patients With Multiple Sclerosis. *Archives of*
772 *Neurology*, 67(4), 447-453. <https://doi.org/10.1001/archneurol.2010.48>
- 773 Peluso, M. J., Kelly, J. D., Lu, S., Goldberg, S. A., Davidson, M. C., Mathur, S., Durstenfeld, M. S.,
774 Spinelli, M. A., Hoh, R., Tai, V., Fehrman, E. A., Torres, L., Hernandez, Y., Williams, M.
775 C., Arreguin, M. I., Bautista, J. A., Ngo, L. H., Deswal, M., Munter, S. E., . . . Martin, J. N.
776 (2021). Rapid implementation of a cohort for the study of post-acute sequelae of
777 SARS-CoV-2 infection/COVID-19. *medRxiv*, 2021.2003.2011.21252311.
778 <https://doi.org/10.1101/2021.03.11.21252311>
- 779 Perica, M. I., Ravindranath, O., Calabro, F. J., Foran, W., & Luna, B. (2021). Hippocampal-
780 Prefrontal Connectivity Prior to the COVID-19 Pandemic Predicts Stress Reactivity.
781 *Biol Psychiatry Glob Open Sci*, 1(4), 283-290.
782 <https://doi.org/10.1016/j.bpsgos.2021.06.010>
- 783 Politi, L. S., Salsano, E., & Grimaldi, M. (2020). Magnetic Resonance Imaging Alteration of the
784 Brain in a Patient With Coronavirus Disease 2019 (COVID-19) and Anosmia. *JAMA*
785 *Neurol*, 77(8), 1028-1029. <https://doi.org/10.1001/jamaneurol.2020.2125>
- 786 Power, J. D., Barnes, K. A., Snyder, A. Z., Schlaggar, B. L., & Petersen, S. E. (2012). Spurious
787 but systematic correlations in functional connectivity MRI networks arise from
788 subject motion. *Neuroimage*, 59(3), 2142-2154.
789 <https://doi.org/10.1016/j.neuroimage.2011.10.018>
- 790 Qin, Y., Wu, J., Chen, T., Li, J., Zhang, G., Wu, D., Zhou, Y., Zheng, N., Cai, A., Ning, Q., Manyande,
791 A., Xu, F., Wang, J., & Zhu, W. (2021). Long-term microstructure and cerebral blood
792 flow changes in patients recovered from COVID-19 without neurological
793 manifestations. *J Clin Invest*, 131(8). <https://doi.org/10.1172/jci147329>
- 794 Raichle, M. E., & Mintun, M. A. (2006). Brain work and brain imaging. *Annu Rev Neurosci*, 29,
795 449-476. <https://doi.org/10.1146/annurev.neuro.29.051605.112819>
- 796 RStudio. (2021). *RStudio Team (2021). RStudio: Integrated Development for R.*
797 <http://www.rstudio.com/>. In RStudio.
- 798 Shirer, W. R., Ryali, S., Rykhlevskaia, E., Menon, V., & Greicius, M. D. (2012). Decoding
799 subject-driven cognitive states with whole-brain connectivity patterns. *Cereb Cortex*,
800 22(1), 158-165. <https://doi.org/10.1093/cercor/bhr099>
- 801 Shulman, R. G., Rothman, D. L., Behar, K. L., & Hyder, F. (2004). Energetic basis of brain
802 activity: implications for neuroimaging. *Trends Neurosci*, 27(8), 489-495.
803 <https://doi.org/10.1016/j.tins.2004.06.005>
- 804 Smith, S. M., Fox, P. T., Miller, K. L., Glahn, D. C., Fox, P. M., Mackay, C. E., Filippini, N.,
805 Watkins, K. E., Toro, R., Laird, A. R., & Beckmann, C. F. (2009). Correspondence of the
806 brain's functional architecture during activation and rest. *Proceedings of the*
807 *National Academy of Sciences*, 106(31), 13040-13045.
808 <https://doi.org/10.1073/pnas.0905267106>
- 809 Soudry, Y., Lemogne, C., Malinvaud, D., Consoli, S. M., & Bonfils, P. (2011). Olfactory system
810 and emotion: Common substrates. *European Annals of Otorhinolaryngology, Head*
811 *and Neck Diseases*, 128(1), 18-23.
812 <https://doi.org/https://doi.org/10.1016/j.anorl.2010.09.007>

- 813 Tabacof, L., Tosto-Mancuso, J., Wood, J., Cortes, M., Kontorovich, A., McCarthy, D., Rizk, D.,
814 Mohammadi, N., Breyman, E., Nasr, L., Kellner, C., & Putrino, D. (2020). Post-acute
815 COVID-19 syndrome negatively impacts health and wellbeing despite less severe
816 acute infection. *medRxiv*, 2020.2011.2004.20226126.
817 <https://doi.org/10.1101/2020.11.04.20226126>
- 818 Taylor, P. A., & Saad, Z. S. (2013). FATCAT: (an efficient) Functional and Tractographic
819 Connectivity Analysis Toolbox. *Brain Connect*, 3(5), 523-535.
820 <https://doi.org/10.1089/brain.2013.0154>
- 821 Tu, Y., Zhang, Y., Li, Y., Zhao, Q., Bi, Y., Lu, X., Kong, Y., Wang, L., Lu, Z., & Hu, L. (2021). Post-
822 traumatic stress symptoms in COVID-19 survivors: a self-report and brain imaging
823 follow-up study. *Molecular Psychiatry*. [https://doi.org/10.1038/s41380-021-01223-](https://doi.org/10.1038/s41380-021-01223-w)
824 [w](https://doi.org/10.1038/s41380-021-01223-w)
- 825 van Schouwenburg, M. R., den Ouden, H. E., & Cools, R. (2015). Selective attentional
826 enhancement and inhibition of fronto-posterior connectivity by the basal ganglia
827 during attention switching. *Cereb Cortex*, 25(6), 1527-1534.
828 <https://doi.org/10.1093/cercor/bht345>
- 829 Wortinger, L. A., Glenne Øie, M., Endestad, T., & Bruun Wyller, V. (2017). Altered right
830 anterior insular connectivity and loss of associated functions in adolescent chronic
831 fatigue syndrome. *PLoS One*, 12(9), e0184325.
832 <https://doi.org/10.1371/journal.pone.0184325>
- 833 Xiao, M., Chen, X., Yi, H., Luo, Y., Yan, Q., Feng, T., He, Q., Lei, X., Qiu, J., & Chen, H. (2021).
834 Stronger functional network connectivity and social support buffer against negative
835 affect during the COVID-19 outbreak and after the pandemic peak. *Neurobiology of*
836 *Stress*, 15, 100418-100418. <https://doi.org/10.1016/j.ynstr.2021.100418>
- 837 Yan, C.-G., Wang, X.-D., Zuo, X.-N., & Zang, Y.-F. (2016). DPABI: Data Processing & Analysis
838 for (Resting-State) Brain Imaging. *Neuroinformatics*, 14(3), 339-351.
839 <https://doi.org/10.1007/s12021-016-9299-4>
- 840 Yeo, B. T., Krienen, F. M., Sepulcre, J., Sabuncu, M. R., Lashkari, D., Hollinshead, M., Roffman,
841 J. L., Smoller, J. W., Zöllei, L., Polimeni, J. R., Fischl, B., Liu, H., & Buckner, R. L. (2011).
842 The organization of the human cerebral cortex estimated by intrinsic functional
843 connectivity. *J Neurophysiol*, 106(3), 1125-1165.
844 <https://doi.org/10.1152/jn.00338.2011>
- 845 Zhang, S., Cui, J., Zhang, Z., Wang, Y., Liu, R., Chen, X., Feng, Y., Zhou, J., Zhou, Y., & Wang, G.
846 (2022). Functional connectivity of amygdala subregions predicts vulnerability to
847 depression following the COVID-19 pandemic. *J Affect Disord*, 297, 421-429.
848 <https://doi.org/10.1016/j.jad.2021.09.107>

849

850

851

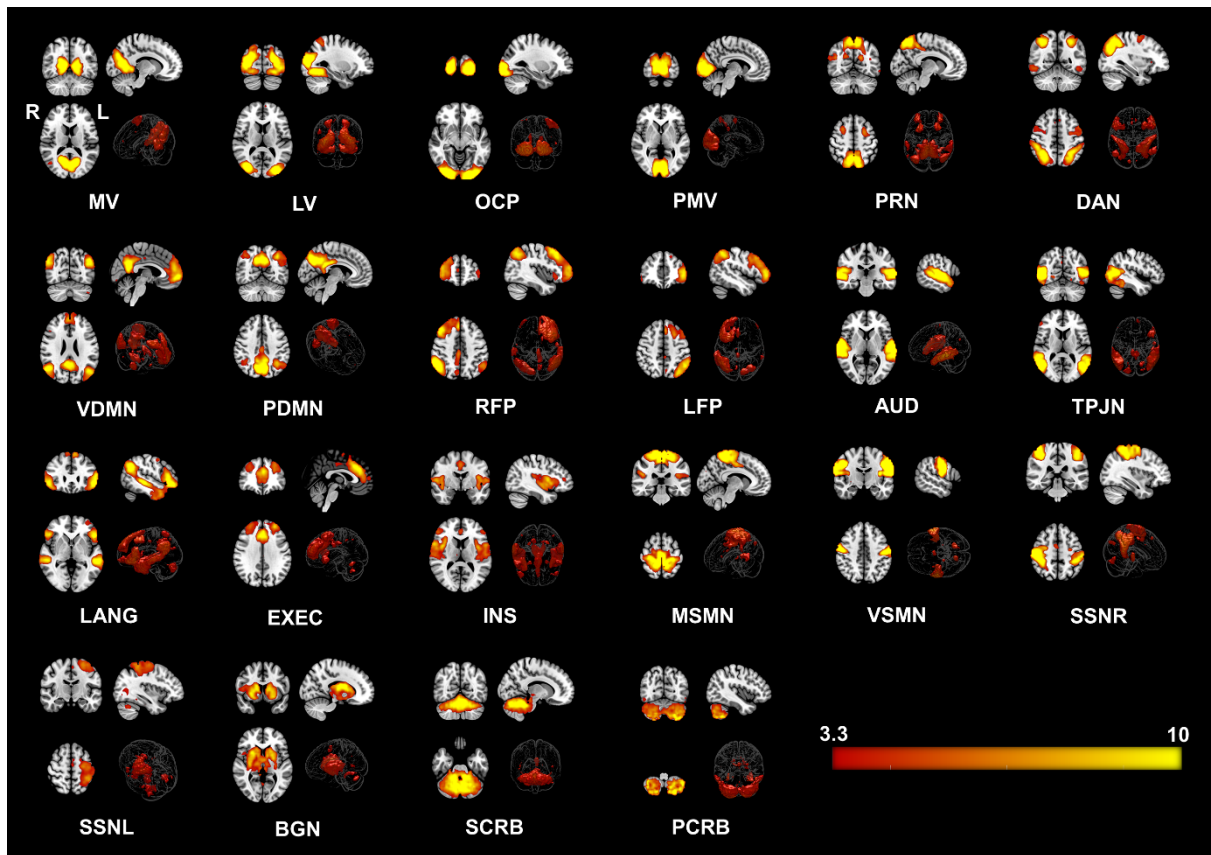


Figure 1. Twenty-two Resting State Networks (RSNs) identified from group ICA using 'melodic'. Abbreviated names of each network are shown at the bottom of each image. Three orthogonal slices are shown for each network along with a volume rendered image to show depth and three-dimensional view of the RSNs. Statistical estimates (Z-scores) are embedded into a colorbar at the bottom-right. **Keys:** MV = Medial Visual, LV = Lateral Visual, OCP = Occipital Pole, PMV = Primary Visual Network, PRN = Precuneus Network, DAN = Dorsal Attention, VDMN = Ventral Default Mode Network (DMN), PDMN = Posterior DMN, RFP = Right Fronto Parietal, LFP = Left Fronto Parietal, AUD = Auditory, TPJN = Temporo-Parietal Junction Network, LANG = Language Network, EXEC = Executive Control Network, INS = Insular Network, MSMN = Medial Sensory-Motor Network (SMN), VSMN = Ventral SMN, SSNR = Somatosensory Network - Right, SMNL = Somatosensory Network - Left, BGN = Basal Ganglia Network, SCRIB = Superior Cerebellar Network, PCRIB = Posterior Cerebellar Network; R = Right Hemisphere of the Brain, L = Left Hemisphere of the Brain.

852

853

854

855

856

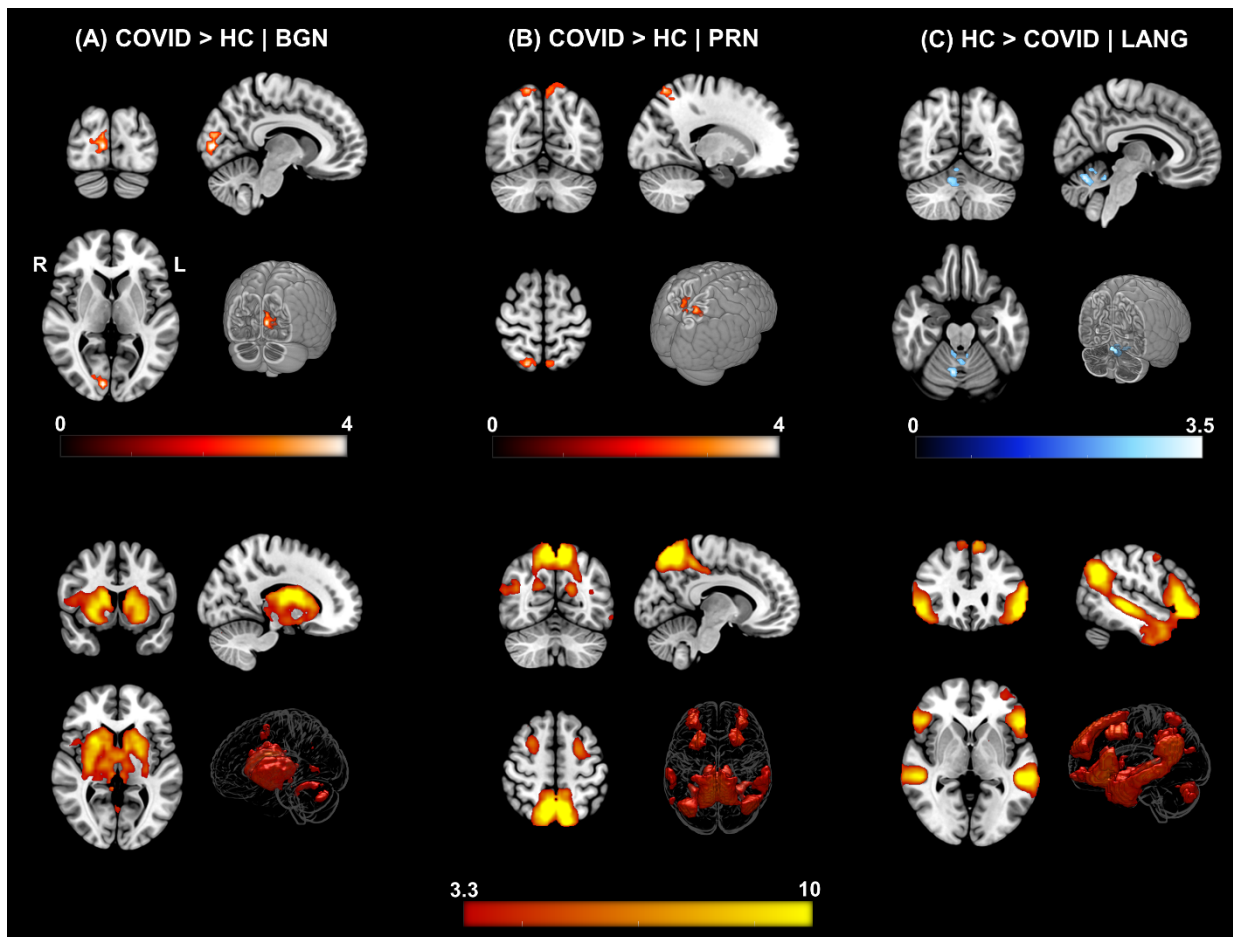


Figure 2. Δ FC | Functional Connectivity differences between COVID survivors and healthy controls. [top row] (A) COVID > HC: Enhanced FC in COVID compared to HCs observed in the *Basal Ganglia Network (BGN)* network. Three orthogonal slices (left) along with a cut-to-depth volume rendered image to show the effects in the *right Calc, Cu and LiG*. The colorbar represents t – score values. Cluster information include - cluster peak: $[9 -84 6]$, and cluster size = 69 voxels. **(B) COVID > HC:** Enhanced FC in COVID compared to HCs observed in the *Precuneus (PRN)* network, demonstrating a significant difference in FC in the *bilateral SPL and PCu* regions. Cluster information include - cluster peak: $[21 -57 54]$ and cluster size = 90 voxels. Please note, enhanced FC among COVID survivors in both **(A)** and **(B)** is represented with a hot iron colormap and corresponding colorbar. **(C) HC > COVID:** Reduced FC in COVID compared to HC group observed in the *Language (LANG)* network demonstrating significant FC differences in several vermal layers of the *Cerebellum*. The electric blue colormap and corresponding colorbar are used to indicate that FC is reduced in the COVID group. Cluster information include - cluster peak: $[9 -63 -24]$ and cluster size = 57 voxels. [bottom row] Corresponding group level ICA networks from which FC differences are shown on the top row. The colorbar represents z-scores.

857

858

859

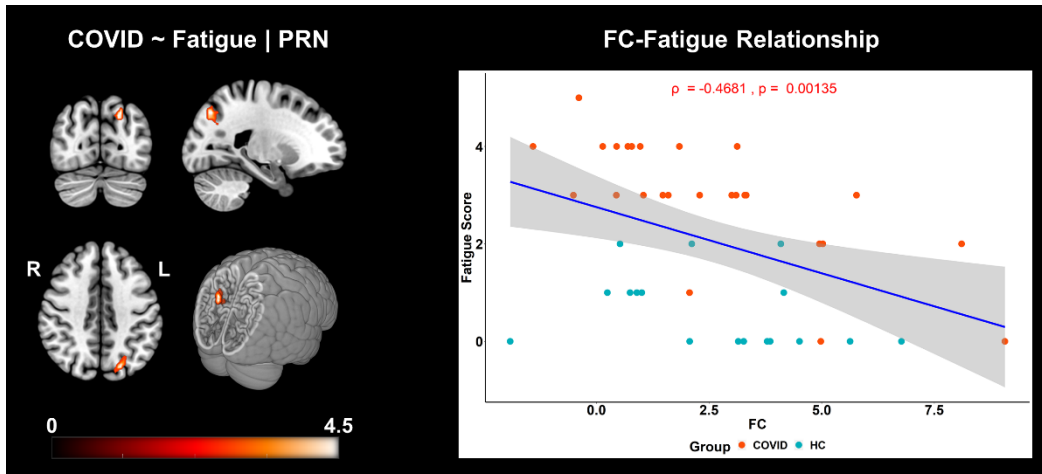


Figure 3. FC is negatively correlated with self-reported fatigue scores in COVID and HC individuals. The three orthogonal slices on the left, shows the cluster withing the *PRN* network, along with a cut-to-depth volume rendered image consisting of *Superior Parietal Lobule (SPL)*, *Superior Occipital Gyrus (SOG)*, *Angular Gyrus (AnG)*, *Precuneus (PCu)*. This cluster demonstrated significantly negative correlation with fatigue. The colorbar represents t-score values. The cluster consisted of 46 voxels and the peak was located at MNI coordinates: $[-21 -72 42]$. The peak t -score of the cluster was, $t_{peak} = 4.40$, and corrected for multiple comparisons by controlling false discovery rates, at $p_{fdr} < 0.05$. The graph on the right shows the linear relationship between FC within the significant cluster and self-reported fatigue scores across all groups. The x-axis represents the residuals plus the average FC (z-scores) across groups from the cluster and the y-axis represents the fatigue scores. The light pink dots represent the COVID group, and the cyan dots represent the HC group. The shaded gray area represents the 95% confidence interval. The blue line represents the least squares regression line of best fit.

860

861

862

863

864

865

866

867

868

869

870

871

873 **Tables**

Clinical Category	Assessment/ Treatment	No. Aff.	No Info.	Data Avail.	No. Tot.	% Out of Avail.	% Out of Total
Symptom Severity	Mild	17	9	38	47	44.74	36.17
	Moderate	4	9	38	47	10.53	8.51
	Moderate-Severe	17	9	38	47	44.74	36.17
Medication & O ₂ Support	Remdesivir	10	9	38	47	26.32	21.28
	Additional O ₂	5	9	38	47	13.16	10.64
	BiPap & Actemra	1	9	38	47	2.63	2.13
	Mix Medications*	1	9	38	47	2.63	2.13
	Antibiotic & Steroid	1	9	38	47	2.63	2.13

Table 1. Clinical information detailed by symptom severity and medical treatment of COVID participants. The table shows the number and percentages of participants based on two clinical categories. The first three rows show number and percentage of participants by symptom severity and the last five rows are based on the type of medication administered and the requirement of O₂ support. Particularly, information from 9 participants could not be obtained as these participants did not agree to share the symptom publicly/anonymously. **Keys:** No. Aff. = number of affected patients, No Info. = no information available because these patients did not give consent to share symptom information, Data Avail. = number of subjects with clinical assessment data available, No. Tot. = total number of patients including those with no information available, % Out of Avail. = proportion of patients affected vs patients with clinical assessment data available (n = 38) in percentages, % Out of Total = proportion of patients affected vs. total number of patients (n = 47) in percentages, O₂ = oxygen supplied to support breathing, BiPap = bilevel positive air pressure, Mix Medications* = a combination of medications – Dexamethasone, Ceftriaxone and Clexane injections

Measures	<i>p</i>	<i>stat</i>	HC, mean (SD)	COVID, mean (SD)
Age (years)	0.66	-0.44 (<i>t</i>)	33.50 (9.74)	34.63 (11.54)
Sex	0.38	0.76 (χ^2)	23M, 7F	31M, 15F
Fatigue	2.097e-07	36.5 (<i>T</i>)	0.65 (0.79)	2.93 (1.21)

875 **Table 2: Group level statistics on participant demographics among HC and COVID**
876 **group.** The table shows the test results from participant demographics including age, sex
and fatigue. There was no significant differences in age and sex between the two groups.
However, the COVID group experienced significantly higher fatigue levels compared to HC
group. **Keys:** *p* = *p-value*, *t* = *two-sample t-test statistic*, χ^2 = *Chi-Squared statistic*, *T* =
Wilcoxon Rank Sum test score, M = Male, F = Female.

877

Δ FC	RSN Name	Cl. No.	Anatomical Locations	Cl. Size	Peak MNI Coordinates			Peak <i>t</i>	p_{FWE}
					X	Y	Z		
COVID > HC	BGN	1	Right – Calcarine Cortex (<i>Calc</i>) Right – Cuneus (<i>Cun</i>) Right – Lingual Gyrus (<i>LiG</i>)	69	9	-84	6	4.46	0.004
	PRN	1	Right – Superior Parietal Lobule (<i>SPL</i>) Right – Precuneus (<i>PCu</i>) Left – Superior Parietal Lobule (<i>SPL</i>) Left – Precuneus (<i>PCu</i>)	90	21	-57	54	4.22	0.001
HC > COVID	LANG	1	Right – Cerebellar Exterior (<i>CExt.</i>) Right – Cerebellar Vermal Lobules I-V Right – Cerebellar Vermal Lobules VI-VII	57	9	-63	-24	3.56	0.019

Table 3. List of spatial regions from significant clusters obtained from the contrast – COVID > HC. The regions from three RSNs – *BGN*, *PRN* and *LANG* which demonstrated significant differences are presented with peak MNI coordinates (X Y Z) and corresponding *peak t*-score values for each cluster. **Keys:** Δ FC = Direction of change in Functional Connectivity; Cl. = Cluster; Cl. No. = Number of Clusters; Cl. Size = Cluster Size; Peak *t* = *peak t*-score; p_{FWE} = family wise error corrected p-value.

878

879

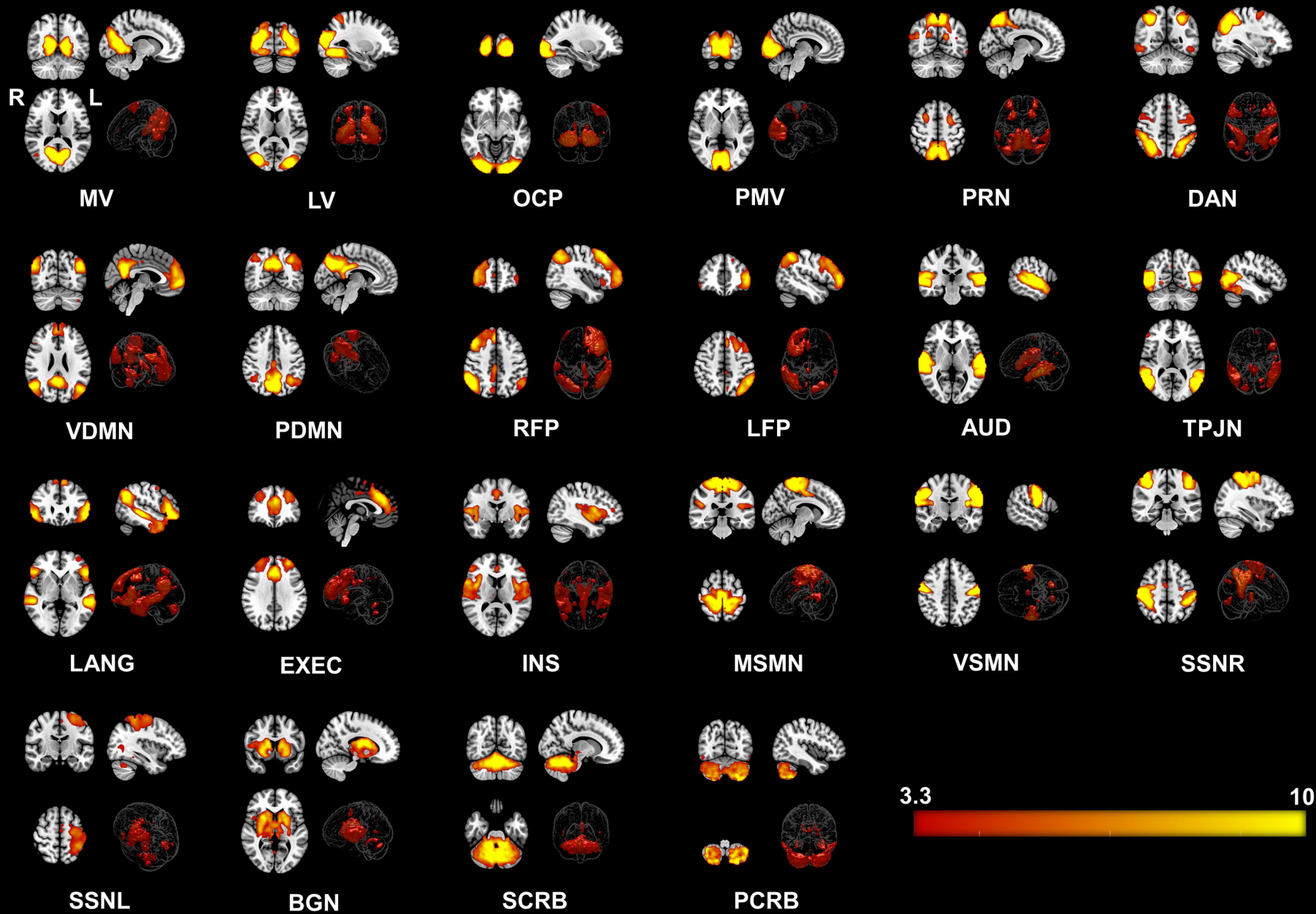
880

Corr (FC, ftg.)	RSN Name	Cl. No.	Anatomical Locations	Cl. Size	Peak MNI Coordinates			Peak <i>t</i>	p_{FDR}
					X	Y	Z		
COVID	PRN	1	Left – Superior Parietal Lobule (SPL) Left – Superior Occipital Gyrus (SOG) Left – Angular Gyrus (AnG) Left – Precuneus (PCu)	46	-21	-72	42	4.40	< 0.05

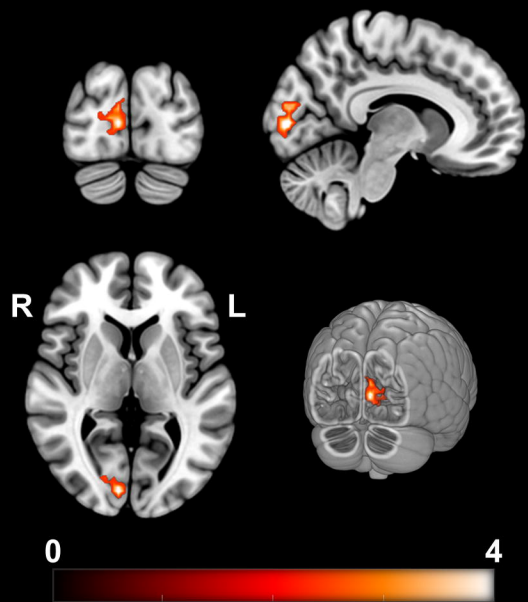
Table 4. List of spatial regions from the cluster showing significant correlation with self-reported fatigue among COVID individuals. The regions from PRN which demonstrated significant correlation are presented with peak MNI coordinates (X Y Z) and corresponding peak *t*-score values for each cluster. **Keys:** FC = Functional Connectivity; ftg. = Fatigue Scores, Cl. = Cluster; Cl. No. = Number of Clusters; Cl. Size = Cluster Size; *t* = peak *t*-score; p_{FDR} = false discovery rate corrected *p*-value.

881

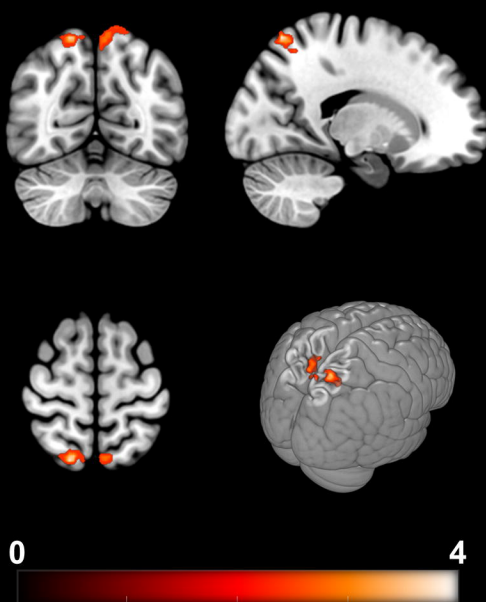
882



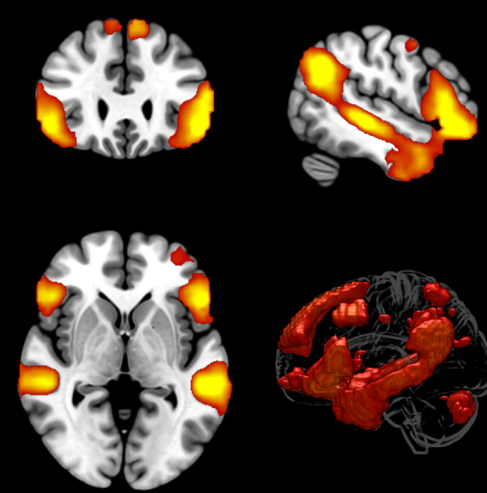
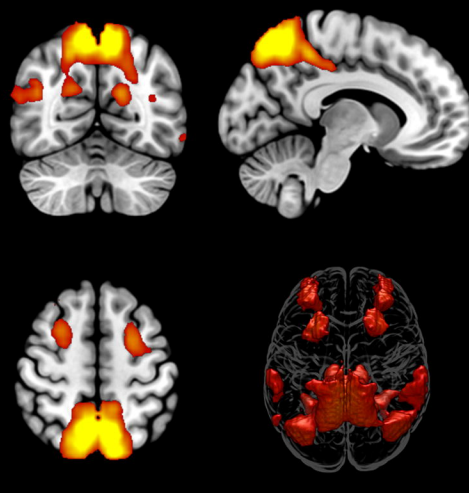
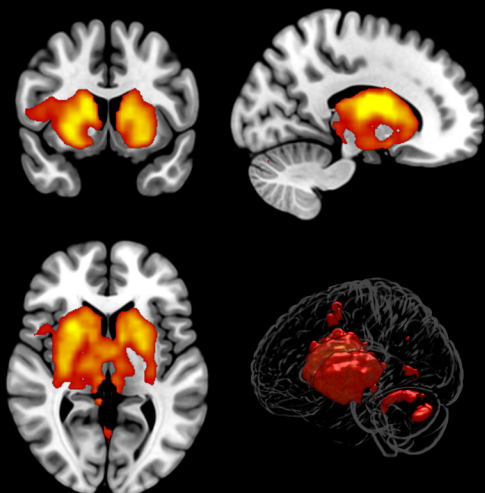
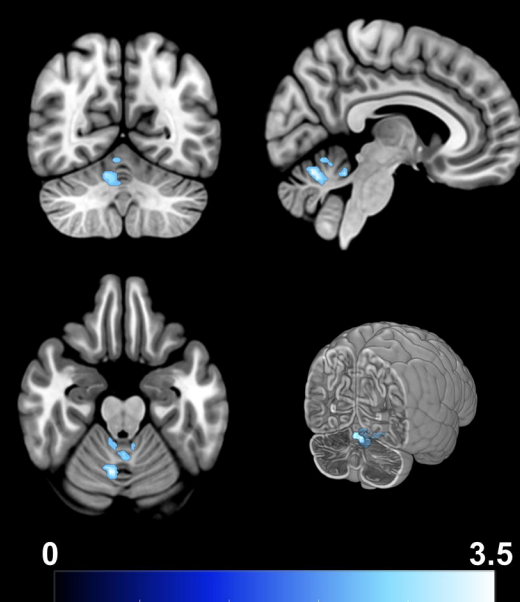
(A) COVID > HC | BGN



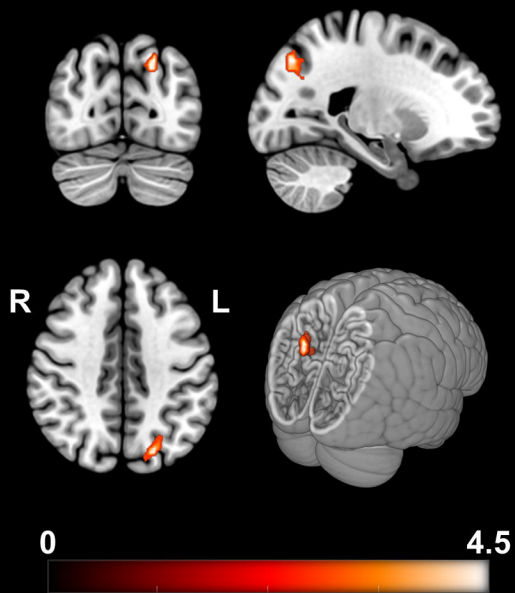
(B) COVID > HC | PRN



(C) HC > COVID | LANG



COVID ~ Fatigue | PRN



FC-Fatigue Relationship

